NOVEL REACTOR FOR THE PRODUCTION OF SYNTHESIS GAS
DOE AWARD # DE-FC26-00NT41027

FINAL TECHNICAL PROGRESS REPORT

Principal Authors: Vasilis Papavassiliou
Principal Investigator: Vasilis Papavassiliou
Program Manager: Vasilis Papavassiliou

Contributors: Leo Bonnell (Foster Wheeler)
    Dion Vlachos (U. Delaware)

DISCLAIMER

ABSTRACT

Praxair investigated an advanced technology for producing synthesis gas from natural gas and oxygen This production process combined the use of a short-reaction time catalyst with Praxair's gas mixing technology to provide a novel reactor system. The program achieved all of the milestones contained in the development plan for Phase I. We were able to develop a reactor configuration that was able to operate at high pressures (up to 19atm). This new reactor technology was used as the basis for a new process for the conversion of natural gas to liquid products (Gas to Liquids or GTL). Economic analysis indicated that the new process could provide a 8-10% cost advantage over conventional technology. The economic prediction although favorable was not encouraging enough for a high risk program like this. Praxair decided to terminate development.

TABLE OF CONTENTS

1. EXECUTIVE SUMMARY

The report summarizes the development effort of a new technology to convert natural to liquid products for the utilization of stranded natural gas. The new technology is based on a technology developed by Praxair and is named the Catalytic Hot Oxygen reactor. This effort was led by Praxair. Foster Wheeler and University of Delaware also participated under respective subcontracts.

Praxair developed a high pressure reactor system (Catalytic Hot O2 Reactor or CHOR) that converts natural gas and O_2 over a precious metal catalyst to a synthesis gas that is suitable for Gas to Liquid applications. This reactor system combines heat generation with natural gas reforming reaction in one step in contrast to autothermal reforming or steam methane reforming were the heat generation step is separate from the reaction step. This reactor system has three components a) thermal nozzle, b) mixing chamber and c) catalyst chamber. Each component has been developed to work at high pressure (up to 20atm) and we are capable of designing a scaled up system for further development. Statistical experiments, computational fluid dynamics and detailed engineering design were used in the development of the system. Several experiments were performed with our high-pressure reactor. We were able to perform experiments that produced synthesis gas up to 19 atm.

Foster Wheeler completed cost and economic evaluation data of the a Gat to Liquids plant based on CHOR technology. This work has initially focused on the preparation of a "baseline" process configuration for a stand-alone facility to produce 25,000 BPSD of distillates from natural gas. The baseline process configuration selected was representative of state-of-the-art commercially available synthesis gas production technology, and as such was an effective yardstick against which the CHOR synthesis gas technology can be measured. The CHOR case exhibited a 8-10% product cost advantage over the base case. The CHOR case consumed less steam, was more thermodynamically efficient and produced more liquid product. The CHOR case was analyzed and further improvements were identified.

In addition to the experimental reactor and process development work University of Delaware (Prof. Dion Vlachos) developed a new reaction mechanism to describe this catalytic system. Most previous work on surface reaction mechanism has violated thermodynamic consistency. What are the implications of thermodynamic inconsistency and why are these important for syngas production were analyzed. This is the first time a systematic approach was developed that can assure full thermodynamic consistency. We focused on preliminary optimization of the methane surface reaction mechanism using the iterative optimization approach. CH_4 conversion as well as CO selectivity predictions were highly improved, whereas H_2 selectivity predictions were improved in the low temperature regime.

Praxair has decided to discontinue this development program. The economic advantage is not sufficient to overcome the considerable risk of developing technology in the GTL area. Praxair will look to license the technology to a more suitable party in the oil and gas industry.

2. INTRODUCTION

A new field of opportunity in catalysis and reaction engineering has recently begun to emerge. This new focus involves high temperature, short reaction time, chemical processes. By operating at high temperatures, reaction times can be greatly reduced and the required reactor size and associated capital cost shrink dramatically. This report details the development of a novel low capital cost reactor for synthesis gas production based on short contact time catalyst and its integration with a Gas to Liquids process. This new reactor utilizes natural gas substantially pure O_2 to produce synthesis gas. Key advantages of this reactor technology are:

- Safe mixing of O_2 and hydrocarbon

- Novel catalyst system for mili-second reaction times with high conversion and selectivity

- Synthesis gas production with 2:1 H_2:CO ratio from natural gas

- No steam addition

This technology is applicable to highly exothermic oxidation reactions, where the heat generated by reaction, H_{Rxn}, provides an immediate heat source such that heat transfer is neither the rate-limiting step nor the high-cost step. The selective oxidation of methane to synthesis gas is an exothermic reaction that can potentially outperform the endothermic steam methane reforming reaction. Encouraging results have been recently obtained by doing selective methane oxidation at short contact times over a Pt or Rh loaded ceramic monoliths[1]. Contrary to the commercial steam methane reforming process, this non-equilibrium process operates autothermally and requires a reaction time three orders of magnitude less than that of the thermal process, and subsequently a much smaller reactor and lower capital costs. Conversion and selectivities exceed 95%.

This new class of reactors utilizing catalytic monoliths was developed by L. Schmidt[2] and his group at University of Minnesota. They used a ceramic monolith coated with a precious metal catalyst (preferably Pt or Rh) and operated at very short contact times (approximately 1-10 millisecond). However, they utilized conventional ways of reactant mixing, which makes their reactor difficult to scale-up to industrially meaningful sizes. For an industrial system appropriate care must be taken so that the hydrocarbon/O_2 stream does not react homogeneously before it reaches the catalyst. In addition a safe way of igniting the catalyst has yet to be invented. Those reactors were able to produce syngas with selectivity for CO 90-95% and selectivity for hydrogen up to 95% while operating at low pressure (few psig). Although with low pressure laboratory reactors pure O_2 addition to natural gas has low risk at larger scale and higher pressures the risk increases considerably.

---

[1] D. A. Hickman and L.D. Schmidt, *Science*, 259 (1993)
[2] Hickman and Schmidt, AIChE Jr. 1993, 1164

Pure O_2 introduces significant challenges to short reaction time catalytic reactor design due to safety and the possibility of initiating run-away reactions. To overcome these limitations, Praxair developed the Catalytic Hot Oxygen Reactor (CHOR). CHOR is based on a patented Praxair thermal nozzle [1] that produces a very high temperature and very high velocity oxygen stream. In the CHOR, this thermal nozzle is combined with a mixing chamber where the hot oxygen rapidly entrains a hydrocarbon feed gas, and a catalyst chamber where a high activity catalyst converts the reaction mixture (at unusually high temperature, pressure, and velocity) into syngas. Because of the rapid mixing and high velocities CHOR can safely handle flammable oxygen-hydrocarbon feed mixtures and operate at reactive conditions that have not been explored previously due to safety limitations.

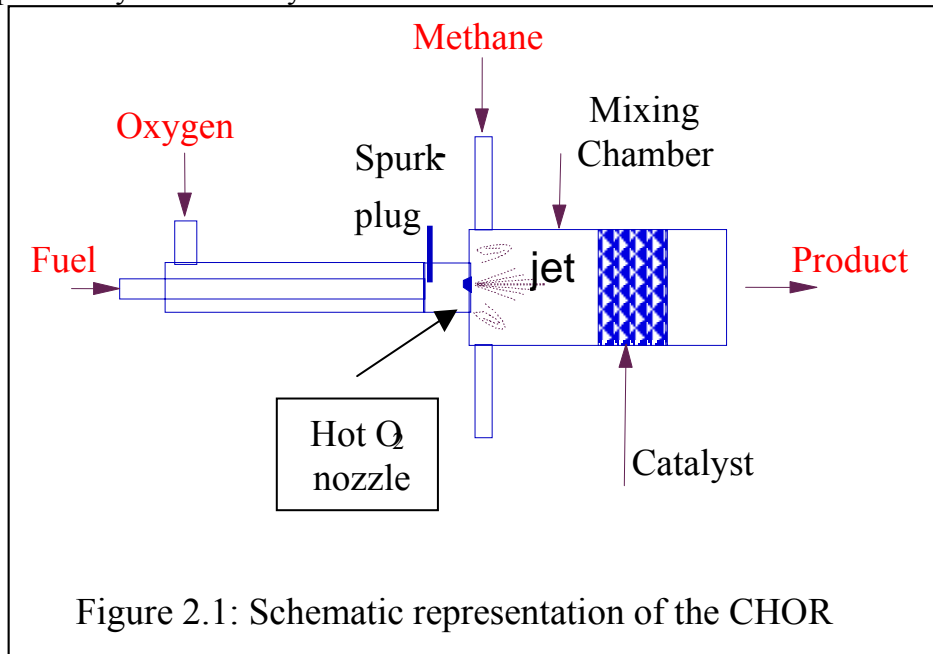Figure 2.1: Schematic representation of the CHOR

Figure 2.1 shows a schematic of the laboratory scale CHOR that Praxair constructed and tested to determine the feasibility of this concept. Praxair has received a patent for this reactor system. The thermal nozzle section of the CHOR is depicted at the left side of Figure 2.1. In this region, a small amount of fuel gas is burned in excess oxygen in a diffusion flame. A spark electrode is used to ignite the flame. The combustion of the fuel gas supplies the energy to heat the unreacted portion of the oxygen stream. The temperature of the hot oxygen stream can be precisely controlled by the amount of fuel fed to the diffusion flame. The velocity of the hot oxygen stream is also related directly to the amount of fuel and the nozzle diameter. Exit velocities of over 400 m/s can easily be obtained. As long as the temperature of the hot oxygen effluent does not exceed 1650 °C, Praxair has demonstrated that the thermal nozzle does not require any external cooling. There are three reasons for the surprising mechanical stability of the thermal nozzle:

1) <u>Low Heat Transfer Rate.</u> Heat transfer from oxy-fuel combustion products to a surface can be very intense because of the presence of active species such as atomic hydrogen and oxygen that recombine on the surface with a high heat of reaction. However, if the temperature is kept below 1650°C, the concentrations of such active species are small.

Therefore, the heat transfer from a hot oxygen stream not exceeding 1650°C to a surface is an order of magnitude lower than that for combustion products from a stochiometric oxy-fuel burner.

2) Cool Oxygen Boundary Layer. There is a cooler boundary layer of oxygen at the perimeter of the hot oxygen stream adjacent to the nozzle surface. Thus, the nozzle surface does not contact the hot oxygen.

3) Small Exposed Heat Transfer Area. The total heat transfer to the nozzle is relatively small.

Once the hot oxygen stream is formed, it is immediately expanded through a nozzle into a mixing chamber where the primary fuel reactant is added. The mixing between the hot oxygen and the feed gas is very rapid due to the density difference between the hot O_2 and the colder fuel gas, and the turbulence introduced by the O_2 jet expansion. This is illustrated in Table 2.1 in which calculated results are presented for the entrainment of methane into an oxygen jet. The time required to entrain methane into the O_2 jet decreases as the nozzle diameter decreases and the jet velocity and temperature increase. By using hot O_2 for a given pressure, both the jet velocity and the jet temperature can be increased. From Table 2.1 we conclude that mixing under 0.06 milliseconds is possible. These mixing times are shorter than ignition induction times [8] so that no flame can be formed and stabilized in the mixing chamber. Thus CHOR can deliver a reaction mixture to the catalyst at velocities and temperatures that are unachievable by other methods.

Temperature (°C)	27	1650	1650	27	1650	1650
Velocity (m/s)	300	300	760	300	300	760
Nozzle diameter (cm)	1.27	1.27	1.27	0.16	0.16	0.16
Jet Length (cm)	1.27	1.27	1.27	3.50	1.40	1.40
Mixing Time (ms)	3.2	1.3	0.51	0.40	0.16	0.06

Table 2.1: Calculated results for the entrainment of methane into an oxygen jet for a 10:1 methane to oxygen ratio based on the entrainment rate equation [9].

The reactive mixture is fed to the catalyst before any significant homogeneous reaction can occur. The reaction on the catalyst is very rapid and highly exothermic. The catalyst chamber combines heat generation with chemical reaction a feature that significantly differentiates this reactor system from conventional technologies such as steam reforming, autothermal reforming and non-catalytic partial oxidation. Suitable catalysts for this process are precious metal catalysts (Pt, Rh, and Pd) supported on ceramic substrates. The ceramic substrate can be in the form of foam or honeycomb monoliths or as conventional pellets. The hot gas produced from the CHOR thermal nozzle provides an efficient way for the catalyst ignition without the requirement of any external heating. By catalyst ignition we mean the initiation of the reaction on the catalytic surface. Catalyst ignition occurs as soon as the catalyst surface is heated above a specific temperature (300-400°C). The temperature of the reaction mixture (hot O_2 and natural gas) depends on the temperature and amount of the hot O_2, and the temperature and amount of the hydrocarbon that are fed to the mixing chamber. The heat that is carried by the hot O_2 can safely heat the reaction mixture at temperatures above the catalyst ignition temperature.

The CHOR concept was the starting point of this development program for a new GTL technology. CHOR does not require CO_2 recycle, or steam and the syngas produced has a H_2:CO ratio of 2:1 that does not need any adjustment. These characteristics differentiate CHOR from existing technology and could potentially lead to a more cost effective synthesis gas production system. This development program utilized experiments, modeling and economic analysis to determine the feasibility of this new GTL technology for utilizing stranded natural gas. Foster Wheeler and University of Delaware joined Praxair in the development program and performed the economic analysis and reaction mechanism development respectively. Key accomplishments were:

1. A reactor system capable of operating up to 19 atm
2. A detailed economic analysis that predicted a 8-10% cost advantage of the CHOR process
3. A new model that is based on a thermodynamically consistent reaction network

3. TECHNICAL RISK

This program contained several areas of technical risk. In ascending order of specificity, there are risks associated with the development of any new oxidation process, reactor design for high pressure and high temperature operations, flammability considerations and safe operating windows, catalyst performance, and integrating CHOR with other process systems in a GTL plant. Each area of technical risk is discussed separately below.

1) CHOR (Reactor) Design for High Pressure and High Temperature Operation: A key aspect of this technology is its ability to operate safely at high temperature and pressure. Although we had a phenomenological and experimental understanding of the mixing and ignition process at low pressures, system behavior at high pressures was uncertain. To design an effective system the thermal nozzle, mixing chamber and catalyst chamber must perform at high pressures. Material selection for the construction of the various reactor parts was also critical, however the compactness of the system allows flexibility in the selection of high performance materials. In addition, the detailed chemistry and reaction mechanism needed to be better defined to operate CHOR under the best possible conditions and design the most effective catalyst configurations.

2) Flammability Considerations: The commercialization of any new technology in oxidation processes is always difficult due to the inherent flammability of these systems and the resulting need to minimize the probability and effect of explosion. The CHOR addresses the issues of flammability in three major ways: 1) rapid mixing and routing of reactants to the catalyst before on-set of homogeneous reaction, 2) reaction mixture linear velocity much greater than the flame speed so homogeneous flames will be difficult to ignite, and 3) small mixing zone, which minimizes the possibility for flashback.

3) Safe Operations (Composition, Temperature Considerations): With these reaction systems, flammability is not the only issue in determining safe operation. For the preferred partial oxidation products, operation is on the fuel rich side of complete combustion and the upper flammability limit [5, 6]. As richer compositions are used, carbon deposition and catalyst deactivation can shut down the reaction. In fact, at thermodynamic equilibrium, this window of operability closes and coking is predicted at all compositions on the rich side of the upper flammability limit. Experimentally, however, there is a finite range of compositions in this non-equilibrium process outside the flammability limits where carbon deposition does not occur [5, 6]. As contact times decrease, the carbon deposition becomes less favored. This increases the size of the accessible window of operability without carbon deposition. Since the CHOR is capable of being operated with velocities two to three orders of magnitude greater than conventional reactors, it will have a correspondingly larger window of operability. Reaction temperature affects the window of operability in high temperature reactors. This temperature typically ranges between 800 and 1200 °C depending on the reactant composition and the level of preheat. If the reaction temperature is too high, the catalyst or reactor may melt and if the temperature is too low, the reaction will extinguish. The CHOR will also have to be operated within these limits.

4) Catalyst performance: Praxair will use metal loaded ceramic monoliths and pellets as the catalyst for the oxidative de-hydrogenation reaction. In previous laboratory studies these catalysts have shown activity in this reaction system. Additionally, the CHOR appears uniquely capable of maximizing the activity and selectivity performance of these catalysts. However, the effects on the catalyst performance at high pressures from variables such as porosity, metal loading, morphology, and length on the reaction chemistry are not well understood. Other issues such as pressure drops and flow maldistribution also need careful consideration in CHOR design. Long term stability and resistance to coking at high pressures are also issues that need to be addressed.

5) Process Integration with other process systems in GTL Plants: In conventional synthesis gas plants, high-grade waste heat is typically used to generate steam and low-grade heat is rejected to ambient using air or water-cooling. The presence of water vapor in the synthesis gas causes both the recoverable waste heat and that needs to be rejected to be high compared to what may be possible with the CHOR. Typically, this result in steam being available in surplus to the amount required for the process. The issue of waste heat management is exacerbated in the case of synthesis gas manufacture for Fischer Tropsch liquids, since the FT process itself is highly exothermic. The net result is that, in synthesis gas systems using the conventional technologies, there is a significant investment in waste heat recovery systems and a large surplus of steam, which has no obvious application due to the lack of consuming plants in locations where natural gas is inexpensive. The proven technologies against which the CHOR needs to be compared are combined SMR/ATR, which is conventional technology for methanol plants up to 4500 tpd (equivalent to 18,000 BPD of Fischer Tropsch liquids), and ATR which is conventionally proposed for Fischer Tropsch plants and is suitable for trains at least as large as 25,000 BPD. Current Fischer Tropsch technology economy of scale requires large units (15,000 barrels per train and upwards). It is possible that a new approach to synthesis gas production, such as CHOR, will enable the economic range of Fischer Tropsch technology to be extended to smaller train sizes and thus be able to exploit smaller gas fields

The primary objective of this program was to build on earlier work with the CHOR concept to develop a new technology capable of safely, economically, and efficiently converting natural gas to synthesis gas for gas to liquids applications. The earlier work demonstrated that this exciting new technology achieves high conversion and selectivities and safe reactor operation at low pressures. In this program Praxair, Foster Wheeler, and University of Delaware systematically explored the full potential of the CHOR through experimentation, modeling and process economics analysis. The development plan that addressed the risk associated with this program is discussed below.

4.   DEVELOPMENT PLAN

The development plan was designed to address all areas of technical risks that were discussed in Chapter 3. The development plan consisted of two Phases. Only Phase I was completed. The development plan Tasks associated with Phase I are discussed below

1) Task 1: Parametric Investigation of Reactor Components
The target was to achieve safe operation and high performance at pressures up to 20 atm. The reactor had to achieve safe operation with no premature homogeneous reaction, and effective performance of the catalyst that results in H2 and CO yields in excess of 95%. Since high-pressure operation has not been tested before, we gradually raised the pressure to ensure safe operation. It should be noted that all the experiments will be performed at semi-pilot scale since our laboratory (see Section 4) was able to operate at flowrates up to 24,000. The thermal nozzle, mixing chamber, and catalyst chamber were tested at gradually higher pressures to ensure efficient operation. The results of this Task are discussed in Chapter 5.1.

2) Task 3: Technical and Economic Evaluation
In Task 3, in parallel to the development of the CHOR itself, economic design of the balance of the synthesis gas system was addressed. The lifecycle costs of supplying synthesis gas for Fischer Tropsch plant from a CHOR were compared to those of competing technologies such as steam methane reforming, autothermal reforming, and non-catalytic partial oxidation. Preliminary designs were be developed for synthesis gas systems for the conventional scale of operation of 25,000 barrels per day equivalent. The development of the design focused on exploiting the distinct advantages of the CHOR in the context of Fischer Tropsch synthesis gas, and demonstrating the advantages compared to conventional technology. In summary this study addressed the following issues:
- Define basic process configuration for syngas system for 25,000 barrels per day of GTL plant
- Develop preliminary process and equipment specifications.
- Develop preliminary engineering design of special equipment
- Develop factorial cost estimate for the syngas system based on the CHOR as well as an equivalent estimate for syngas systems based on conventional technologies for comparison.
- Develop life cycle cost of production for the CHOR as well as the alternatives.

The results of this work are presented in Chapter 5.2 and a detailed report from Foster Wheeler is included in the Appendix

3) Task 5: Flammability Modeling and Reaction Mechanism Studies
To fully understand the CHOR system, a fundamental reaction/reactor model needed to be developed that included homogeneous and heterogeneous ignition studies and parametric evaluation of reaction mechanisms. This work was performed by Dr. Vlachos and his team at the University of Delaware. The results are described in Chapter 5.3.

5. DEVELOPMENT RESULTS

5.1 Parametric Investigation of reactor components (Task 1)

As described in the development plan as part of Task 1 Praxair tested the thermal nozzle, mixing chamber and catalyst at gradually higher pressures, starting at 5 atm and then 10, 15, and finally 20 atm. The first step in evaluating high pressure operation of the CHOR was developing a thermal nozzle component that can operate at high pressures. Both experiments and computational fluid dynamic (CFD) modeling were used to identify the parameters that are critical in the high pressure thermal nozzle design. Subsequently we developed a high pressure mixing chamber using again a combination of experiments and CFD modeling. Finally the catalyst chamber was developed and operated at high pressure. These three sub-tasks are discussed in paragraphs 5.1.1-3.

5.1.1 High Pressure Thermal Nozzle Development (Task 1.1)

The thermal nozzle operates by combusting a small amount of fuel (up to 8%) in excess O_2 and then expanding the hot O_2 gas through a converging diverging nozzle to form a supersonic turbulent jet. The hot O_2 temperature can be as high as 1600C. Before the onset of this work Praxair had successfully tested the thermal nozzle at relatively low pressures (<60psig). This program needed to develop a reactor that operates at 300psi which meant that the thermal nozzle must operate at about 600psi which is ten times higher than what we had operated before. We performed both modeling and experiments to extend our understanding of the operation of the thermal nozzle at high pressures, which resulted in the redesign of the thermal nozzle apparatus.

Initial experiments were performed with the original thermal nozzle design and where limited to a pressure of up to 200psig. The initial experiments focused in identifying temperature sensitive areas of the thermal nozzle by placing thermocouples at various locations. These temperature measurements demonstrated that nozzle geometry and operating conditions play an extremely important role in determining ultimate steady state thermal nozzle temperatures and, consequently, the safety of this system. As a result, further experiments and CFD modeling of the thermal nozzle were performed to investigate heat transfer in the thermal nozzle while developing a fundamental understanding of the nozzle dynamics and tools for designing safe and optimum high pressure thermal nozzles. The CFD modeling combined turbulent mass transfer, with a simple reaction network to model the heat released during the combustion of the fuel in the thermal nozzle. The results of the CFD modeling were complemented by a statistical analysis (design of experiment) of several factors that affect thermal nozzle operation. It was concluded from the analysis that pressure is the more critical operating parameter. Based on the results a high pressure thermal nozzle was designed, constructed and tested. The thermal nozzle has operated up to 600psig, achieving the first of the technical milestones associated with this program. The development work is discussed in detail in the Appendix.

5.1.2 High pressure mixing chamber development (Task 1.2)

A critical part of our process is the rapid mixing of the hot oxygen gas produced by the thermal nozzle with the natural gas. It is important to produce a homogeneous reactant mixture without initiating homogenous reaction. Mixing in our process is based on the entrainment rate of the expanding hot O_2 jet. A typical configuration to expand the gas is a converging nozzle (Figure 5.1).

Figure 5.1 Convergent nozzle

P_0
ρ_0
T_0
fixed

P_b
can be
varied
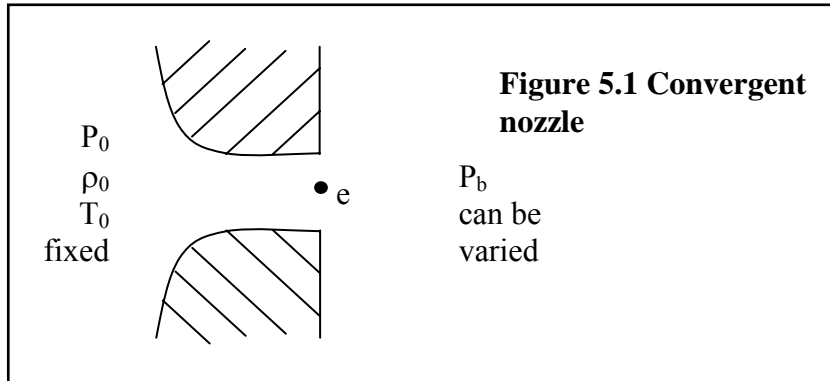
The faster the entrainment rate the faster the mixing. The entrainment rate for non-isothermal jets is described by the following equation[3]:

$$\frac{m}{m_0} \approx \frac{x}{d_0}\left(\frac{\rho}{\rho_0}\right)^{0.5} \qquad (5.1)$$

where:

m is the flowrate that is entrained into the jet

m_0 is the flow rate of the jet at the nozzle exit

x is the distance from the nozzle exit

d_0 is the nozzle diameter

ρ is the density of the gas that is entrained into the jet and

ρ_0 is the density of the jet at the nozzle exit

The density of a gas has an inverse relationship with temperature (ideal gas law). So if the jet gas is at the same temperature as the entrained gas the ratio of densities (ρ / ρ_0) in equation 1 reduces to a constant equal to the ratio of the molecular weights of the two gases. If however the

---

[3] Ricou and Spalding, J. Fluid Mechanics, Vol. II, 1961.

jet gas is at a temperature that is higher that of the entrained gas the mixing is enhanced by a factor equal to the square root of the ratio of the temperatures of the two gases. Faster mixing allows flammable gases to be mixed before the onset of homogeneous reactions. It is obvious from equation (1) that if the jet is at lower temperature than the entrained gas the mixing efficiency decreases. In equation 5.1 the entrainment rate is also proportional to the nozzle diameter (d_0). The diameter of the nozzle is determined by the sonic velocity limitation. Higher hot gas temperatures correspond to higher sonic velocities so a smaller nozzle diameter can be used to accommodate the same flow rate. Smaller nozzle diameter increases the entrainment rate (Equation 5.1).

The hot gas that is produced from the thermal nozzle is expected to entrain the primary fuel which is added at the base of hot gas jet. The initial design of the high pressure mixing chamber was based on the low pressure reactor and was appropriately designed to connect to the thermal nozzle. Using that design the mixing chamber performance was tested at progressively higher pressures. We found that behavior at high pressure was significantly different than that observed at low pressure. The initial design of the mixing chamber failed to operate above 50psig at the desired O_2:CH_4 ratio of 1:2. Although, at low pressure, operation was smooth as pressure increases the temperature at the exit of the mixing chamber increases indicating the onset of homogeneous reactions. Computational fluid dynamics (CFD) simulations were performed next to understand the route of the problem. The CFD simulation revealed that mixing changes drastically at higher pressures and a recirculation zone at the base of the jet caused delayed mixing that likely contributed to flame stabilization at the base of the jet. CFD also indicated that simple design changes could restore operation to the desirable conditions.

The mixing chamber was redesigned and tested for pressures up to 250psig. The redesigned mixing chamber did not exhibit any temperature deviations from expected performance. The details of the mixing chamber design are given in the Appendix. The new mixing chamber was then used in the full reactor experiments.

5.1.3   *High pressure catalyst- chamber development (Task 1.3)*

Lanny Schmidt and the University of Minnesota pioneered catalytic partial oxidation reactors[4] utilizing foam monolith catalyst. They used foam ceramic monoliths coated with precious metals by wet impregnation techniques. Generally the metal represents 2-10% of the foam monolith weight. Rhodium on alumina was found to be the most active and selective metal-support combination. In our work we tested both foam and pellet catalyst and combinations of the two to determine the optimum configuration. Several thermocouples were placed along the axis of the catalyst bed. The reactor effluent was analyzed by a gas chromatogrph. The carbon and H_2 mass balances were calculated from the inlet gas flows and dry gas composition analysis of the product stream. The O_2 was used as the reference compound. H_2 selectivity is calculated by:

---

[4] Hickman and Schmidt, AIChE Jr. 1993, 1164

$$Selectivity_{H_2} = \frac{[H_2]}{[H_2]+[H_2O]} \qquad\qquad 5.2$$

where, [C] denotes concentration.

Selectivity to CO is calculated by:

$$Selectivity_{CO} = \frac{[CO]}{[CO]+[CO_2]+\sum_i [Ci]} \qquad 5.3$$

where C_i denotes the concentration of hydrocarbons.

Conversions of methane and O_2 are calculated by:

$$Conversion_{O_2} = \frac{Oxygen([O_2])_{in} - Oxygen([O_2],[CO],[CO_2])_{out}}{Oxygen([O_2])_{in}} \quad 5.4$$

$$Conversion_{CH_4} = \frac{[C H_4]_{in} - [C H_8]_{out}}{[C H_4]_{in}} \qquad\qquad 5.5$$

Conversion and selectivity are indicators of catalyst performance.

The O_2/methane mixture at the exit of the mixing chamber is fed to the catalyst chamber where the partial oxidation reaction takes place. Initial experiments were limited to relatively low pressures (50-100psig). The catalyst was insulated with several inches of ceramic insulation and was placed inside a stainless steel shell that was specifically designed for high pressure operation. The reactor was hydro-tested at high pressures to ensure robust construction. The reactor was brought up to temperature by utilizing heat from the hot O_2. During start up the natural gas to O_2 ratio was kept well above 2 and the pressure was kept around atmospheric. After the catalyst ignited the natural gas to O_2 ratio was adjusted to 2 and the reactor pressure was increased by closing a pressure control valve downstream of the reactor.

During initial experiments we were able to operate at pressures up to 100psig. However above that pressure we observed rapid deterioration in reactor performance with increasingly high temperatures observed on the catalyst bed. The high temperatures indicated that homogeneous reaction start to predominate on the catalyst itself. The solution came by alteration of the catalyst bed design (details in the Appendix). The reactor with the new catalyst bed was able to operate up to 19atm with good conversion and selectivity (>80%). We feel confident that the reactor can be operated at higher pressures and we have developed designs that will achieve that. Given the time and resources limitations at the end of the project we were not able to test the improved design to confirm our expectations. However based on experimental observations and the understanding that has been gained we believe that the reactor can be operated safely for product pressures up to 20atm.

5.2   Technical and Economic Assessment (Task 3)

This work was performed by Foster Wheeler. The Foster Wheeler final report is included in the Appendix and only a summary of the work and major conclusions are discussed in this paragraph. This work focused on the preparation of a "baseline" process configuration for a stand-alone facility to produce 25,000 BPSD of distillates from natural gas and compared it with a case based on the CHOR reactor. The baseline process configuration selected was representative of state-of-the-art commercially available synthesis gas production technology, and as such should be an effective yardstick against which the CHOR synthesis gas technology can be measured. Evaluation of the baseline configuration can also yield important clues about how CHOR can be used to best advantage in this application.

A preliminary selection of the baseline configuration is shown in the block flow diagram Figure A12. The configuration includes the following process steps:

a) Autothermal reforming (ATR) of natural gas with oxygen and steam, at a low (0.6:1) steam to carbon ratio, to produce synthesis gas with a slight excess of hydrogen;
b) Fischer-Tropsch (F-T) slurry-phase reactor to convert the synthesis gas into paraffins and olefins, primarily C20+ waxes;
c) Recycle of unconverted synthesis gas to the ATR and/or the F-T reactors;
d) Recovery of excess hydrogen with gas separation membranes;
e) Hydrotreatment of the F-T product waxes into transportation quality diesel, along with some lighter naphtha and kerosene-range distillates;
f) Electric power generation with a gas turbine, utilizing excess fuel gas; and
g) Oxygen production via cryogenic air separation.

Process data for calculation of heat and material balances, including reactor yields, have been obtained from a variety of non-proprietary sources. The thermal efficiency of the baseline case, defined as the gross heating value of the liquid products divided by the gross heating value of the natural gas feed, was calculated to be 62%.
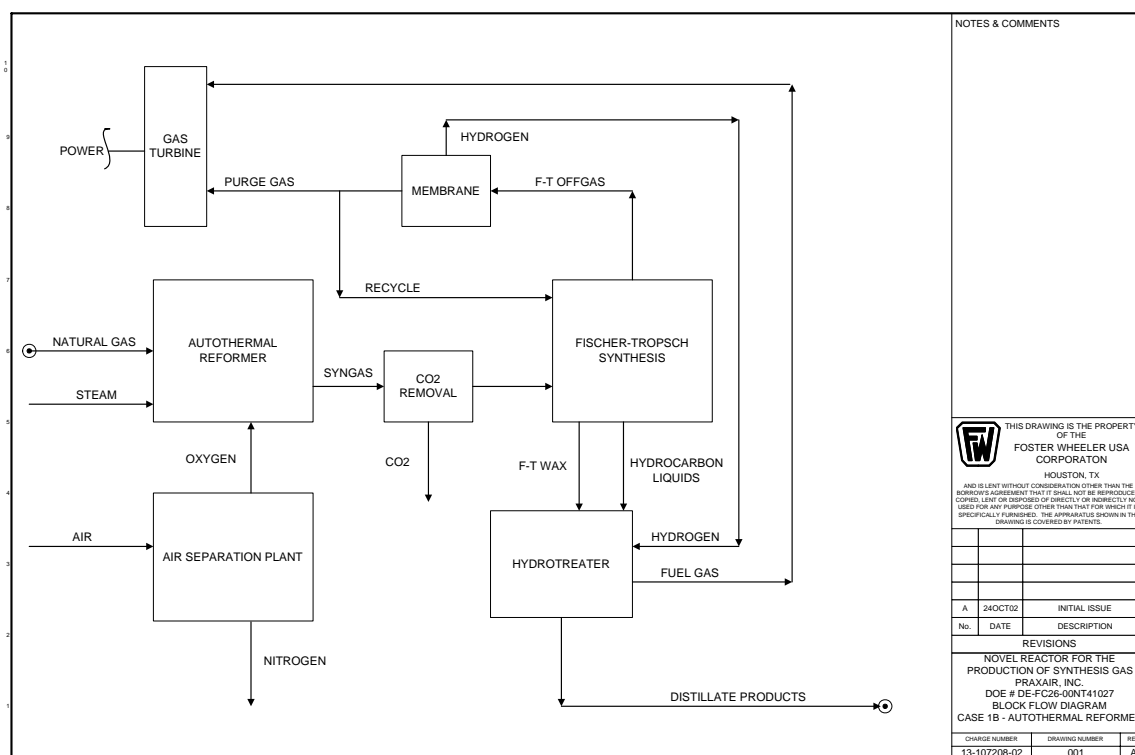
Figure A12. Baseline configuration block flow diagram

Foster Wheeler developed cost and economic estimated of two cases. One case was based on a conventional autothermal reformer and the other case was based on a CHOR reactor. Foster Wheeler developed process flow schemes, using literature information for F-T and Hydro-isomerization sections with no licensor input. Foster Wheeler prepared several process configurations based on CHOR. Foster Wheeler then selected most promising CHOR flow schemes for evaluation and developed simulations (PRO-II) for both cases. Foster Wheeler developed factorial capital estimates for cases and simplified economics for cases. Here are the assumptions of the economic analysis.

1) Generic marine tropical location (location factor 115%)
2) Natural Gas 250MMSCFD
3) Maintenance 3% ISBL capital
4) Plant overhead 70% Direct Fixed Cost
5) Insurance/Property taxes 1% Total Plant Capital
6) Environmental 0.5% Total Plant Capital
7) Return on investment 10% of ISBL and 5% OSBL
8) Depreciation 10% total capital investment

Listed below are the conclusions of the economic analysis
1) CHOR shows $2.30/bbl or 9% overall cost advantage relative to base case
2) CHOR process total capital cost is 10.6% lower
3) CHOR uses 20% less steam
4) CHOR process uses 4% less O2
5) CHOR process produces 2.% more liquids

6) CHOR process thermal efficiency is 62.3% versus 61.2% for the base case (LHV basis)

A detailed report of the work is given the Appendix.

5.3 Flammability Modeling and Reaction Mechanism Studies (Task 4)

The Flammability Modeling work was performed at the University of Delaware under the supervision of Professor Dionisios Vlachos. A summary of the work is presented here but more details can be found in the papers that resulted from this work and are listed in Paragraph 5.3.3.

Most previous work on surface reaction mechanism has violated thermodynamic consistency. Here we review developments for alleviating this long-standing problem, which we think are important for the modeling of syngas production from natural gas. What are the implications of thermodynamic inconsistency and why are these important for syngas production? Aside from the fundamental problem of violation of thermodynamics, thermodynamic consistency of a mechanism plays an important role in calculations involving energetics, where a net nonzero release or consumption of heat (exothermic or endothermic reactions) over a complete cycle of a mechanism can result in errors when energy balances are used. Temperature errors in turn lead to wrong predictions of heat exchange and conversion/selectivity in non-isothermal simulations. Furthermore, errors in enthalpy conservation exponentially propagate to the equilibrium constant, which can significantly affect the equilibrium conversion. The same is true for entropy changes.

An elementary chemical reaction is represented as

$$R_i = \sum_{k=1}^{K_s} v_{ik} A_k = 0, \ i=1,\ldots,K_r$$

where A_k stands for the chemical formula of species k, v_{ik} is the stoichiometric coefficient of species k in reaction i, and K_s is the number of species. Enthalpic conservation at the *single reaction level* means that

$$E_i^{rev} = E_i^{for} - \Delta H_i^0$$

where E_i^{rev}, E_i^{for} are the backward and forward activation energies of reaction i, respectively, and ΔH_i^0 is the heat of ith reaction at standard state. In most mechanisms, the heat of surface reactions is computed from the above equation. However, this does not necessarily assure thermodynamic consistency of catalytic cycles, such as the overall reaction, as elaborated below.

Any catalytic reaction, including the overall reaction, can be obtained by a linear combination of elementary steps

$$R_{cycle} = \sum_i \sigma_i R_i = 0,$$

where σ_i is the coefficient in the linear combination of the elementary steps that leads to the desired stoichiometric reaction and the summation extends over some or all K_r elementary reactions. From Hess law, the appropriate sum of the activation energies for all elementary reaction paths leading from reactants to products must equal the heat of the net (overall) reaction. For any *catalytic cycle level*, the condition for enthalpic consistency is:

$$\Delta H_{cycle}^0 = \sum_i \sigma_i \Delta H_i^0 = \sum_i \sigma_i E_i^{for} - \sum_i \sigma_i E_i^{rev}$$

where ΔH_{cycle}^0 is the heat of a cycle at standard state. The last equation requires that for any reaction cycle (linear combination of surface reactions), the heat must be correct. There are numerous linear combinations for a large number of surface reactions. How many cycles should one consider to assure thermodynamic consistency, and if the latter is violated, how does one correct the situation?

A key issue in thermodynamic consistency of surface reaction mechanisms is the realization that heats of surface reactions are linear combinations of heats of formation of surface species, i.e., the number of independent degrees of freedom is equal to the number of surface species. Thus, if one assures thermodynamic consistency of K_s cycles, the rest should be fine. Our surface reaction mechanisms for oxidation of H_2 [1], CO [2], and CH_4 [3] are developed in such a way that semi-empirical tools like Bond Order Conservation (BOC) [4, 5] and quantum mechanical tools like Density Functional Theory (DFT) become the foundations for calculation of heats of chemisorption, i.e., a multiscale approach is employed in mechanism development that enables one to replace semi-empirical estimates or experimental values with more fundamentally based quantities from quantum-mechanical simulations. A second advantage of our approach is that since our activation energies are calculated using BOC based on the heats of chemisorption of surface species, our methodology has resolved a long-standing problem, namely our mechanism remains consistent on the enthalpic level, at least at room temperature.

The second aspect of thermodynamic consistency is associated with entropy changes, which is often violated in all mechanisms at both the single reaction and the cycle level. In any reversible reaction, the forward and backward pre-exponential factors are related to each other via the entropy of reaction. The equilibrium constant for any reaction in gas phase should be equal to the product of equilibrium constants of individual surface reaction steps, whose linear combination leads to the same stoichiometry, raised to the appropriate power. The conditions for entropic consistency are:

$$A_i^{rev} = A_i^{for} e^{\frac{\Delta G_i^0 - \Delta H_i^0}{RT}} = A_i^{for} e^{\frac{\Delta S_i^0}{R}}$$

$$\prod_i \left(\frac{A_i^{rev}}{A_i^{for}} \right)^{\sigma_i} = e^{\frac{\Delta G_{cycle}^i - \Delta H_{cycle}^i}{RT}} = e^{\frac{\Delta S_{cycle}^i}{R}}$$

where, A_i^{rev} and A_i^{for} are the backward and forward pre-exponential factors of reaction i, ΔG_i^0 is Gibb's free energy of the ith reaction at standard state, ΔS_i^0 is the corresponding entropy change, and ΔG_{cycle}^0 is Gibb's free energy of the reaction cycle at standard state. The equilibrium constant is

$$K_{eq} = e^{-\Delta G_i^0 / RT} = e^{-\Delta H_i^0 / RT} e^{\Delta S_i^0 / R} = K_{eq_H} K_{eq_S},$$

where K_{eq_H} and K_{eq_S} are defined as the enthalpic and entropic contributions to the equilibrium constant, respectively.

The unoptimized mechanism for H_2 oxidation on Pt [1] has been checked for entropic consistency. For a total of 5 cycles in the mechanism, it was found that entropic part of the equilibrium constant is drastically inconsistent from the actual gas phase counterpart. To overcome this difficulty, we have reformulated the optimization problem by minimizing the distance of model predictions from experimental data and of the entropies of catalytic cycles from their gas phase counterpart. This is the first time a systematic approach is developed that can assure full thermodynamic consistency, at least at a certain (room) temperature.

As an example, pre-exponential factors in the H_2 mechanism steps were optimized against LIF data of [6], with additional constraints for entropy conservation. The pre-exponential factors for surface reactions have a bigger uncertainty range than their gaseous reactions; hence, appropriate ranges were assigned to them according to the type of reaction [7]. Due to large variations in pre-exponential factors, the important (active) parameters change, and thus approximate model response with low degree polynomials [8] has not been attempted yet. Instead, we implemented a full model optimization of the mechanism using simulated annealing [9]. Final performance of the mechanism is shown in Figure 5.1. This mechanism was checked for entropic consistency and the comparison is shown in Table 5.1. The mechanism is shown in Table 5.2, and it has been validated against different experimental conditions.

Our approach clearly demonstrates the possibility of maintaining thermodynamic consistency while predicting well experimental data. We believe that assurance of thermodynamic consistency is an important step towards foundation of theoretically sound mechanisms of syngas formation. We currently work on properly including temperature effects within the thermodynamically consistent framework.
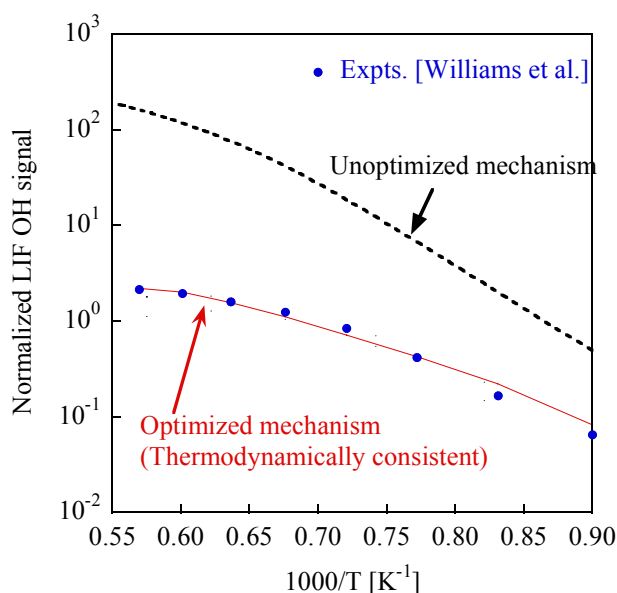

Fig. 5.1: Experimental LIF data [6] and model predictions. Unoptimized mechanism [1] is shown with a dotted line, whereas, the optimized mechanism is shown in solid line. Full thermodynamic consistency is now ensured in the optimized mechanism. The conditions are reactor pressure of 0.2 Torr of H_2O and 0.3 Torr of O_2.

Table 5.1: Comparison of entropic consistency for unoptimized mechanism as well as optimized mechanism for 5 reaction loops in the mechanism. In all cycles, the entropy is

	ΔS (kcal/mole K)	Entropic contribution to Equil. Const., K_{eq_S}
Reaction: $H_2 \leftrightarrow 2H$	**0.028**	**$1.4\ 10^6$**
Unoptimized mechanism	0.019	$1.5\ 10^4$
Optimized mechanism	0.028	$1.4\ 10^6$
Reaction: $O_2 \leftrightarrow 2O$	**0.032**	**$8.1\ 10^6$**
Unoptimized mechanism	0.017	$6.1\ 10^3$
Optimized mechanism	0.031	$7.2\ 10^6$
Reaction: $OH \leftrightarrow O + H$	**0.026**	**$6.0\ 10^5$**
Unoptimized mechanism	0.019	$2.1\ 10^4$
Optimized mechanism	0.027	$6.7\ 10^5$
Reaction: $H_2O \leftrightarrow OH + H$	**0.031**	**$6.2\ 10^6$**
Unoptimized mechanism	0.019	$1.5\ 10^4$
Optimized mechanism	0.031	$5.7\ 10^6$
Reaction: $2H_2 + O_2 \leftrightarrow 2H_2O$	**-0.027**	**$1.1\ 10^{-6}$**
Unoptimized mechanism	-0.022	$1.5\ 10^{-5}$
Optimized mechanism	-0.028	$9.2\ 10^{-7}$

Table 5.2: Entropically consistent surface reaction mechanism for oxidation of H_2 on polycrystalline Pt. The activation energies are in kcal/mol, calculated at zero coverage conditions. Pre-exponentials are in s^{-1} or refer to sticking coefficients for adsorption steps.

No.	Reaction	Unoptimized A or s	E	Optimized A or s
1	$H_2 + 2^* \rightarrow 2H^*$	1.00	0.0	1.00
2	$2H^* \rightarrow H_2 + 2^*$	$1.00\ 10^{13}$	20.0	$3.12\ 10^{12}$
3	$O_2 + 2^* \rightarrow 2O^*$	0.10	0.0	0.06
4	$2O^* \rightarrow O_2 + 2^*$	$1.00\ 10^{13}$	51.0	$5.75\ 10^{14}$
5	$OH^* + ^* \rightarrow H^* + O^*$	$1.00\ 10^{11}$	24.4	$4.59\ 10^{12}$
6	$H^* + O^* \rightarrow OH^* + ^*$	$1.00\ 10^{11}$	12.1	$4.63\ 10^{11}$
7	$H_2O^* + ^* \rightarrow H^* + OH^*$	$1.00\ 10^{11}$	18.4	$2.65\ 10^{10}$
8	$H^* + OH^* \rightarrow H_2O^* + ^*$	$1.00\ 10^{11}$	12.4	$2.18\ 10^{10}$
9	$H_2O^* + O^* \rightarrow 2OH^*$	$1.00\ 10^{11}$	12.6	$1.35\ 10^{10}$
10	$2OH^* \rightarrow H_2O^* + O^*$	$1.00\ 10^{11}$	18.9	$9.07\ 10^{10}$
11	$OH + ^* \rightarrow OH^*$	1.00	0.0	0.01
12	$OH^* \rightarrow OH + ^*$	$1.00\ 10^{13}$	63.0	$5.66\ 10^{13}$
13	$H_2O + ^* \rightarrow H_2O^*$	0.70	0.0	0.11

14	$H_2O^* \rightarrow H_2O + ^*$	$1.00 \ 10^{13}$	10.0	$1.55 \ 10^{13}$
15	$H + ^* \rightarrow H^*$	1.00	0.0	0.07
16	$H^* \rightarrow H + ^*$	$1.00 \ 10^{13}$	60.2	$3.51 \ 10^{12}$
17	$O + ^* \rightarrow O^*$	1.00	0.0	0.45
18	$O^* \rightarrow O + ^*$	$1.00 \ 10^{13}$	92.6	$1.58 \ 10^{15}$

5.3.1   *Quantum mechanical calculations for methane oxidation using DFT*

Following up our previous work, we have continued to work on quantum mechanical calculations using DFT. We have computed heats of adsorption of additional species present in the methane oxidation mechanism. The primary purpose of our DFT calculations is to verify the input of heats of chemisorptions to the mechanism. The comparison of typical DFT calculations as well as BOC calculations is shown in Table 5.3. DFT can also serve as a tool to calculate heats of chemisorption for species like oxygenates, for which experimental information is not available. We plan to introduce oxygenates in the present mechanism and towards this direction, we have started DFT calculations for oxygenates, the comparison of which is again shown in Table 5.3.

Table 5.3: Typical comparison of heats of chemisorption on Pt(111) using DFT as well as BOC. Two oxygenated species are shown in the last two rows of the table.

Species	Q_{DFT} (kcal/mole)	Q_{BOC} (kcal/mole)
C	145.4	150.0
CH_3	42.0	38.0
CH_2	72.9	68.0
H_2O	12.2	10.0
H	55.3	60.2
OH	37.4	38.0
OCH_3	32.8	41.3
OCH_2	7.9	11.4

In addition to Pt(111), Pt(110) surface can also have some contribution to polycrystalline Pt, and more importantly, UHV data (the only ones available) exist from King's group [10]. Currently, we have built a cluster of 30 Pt atoms representing the Pt(110) surface. The new cluster is shown in Figure 5.2. We expect to finish optimization of heats of adsorption of various species on Pt(110) in the near future. Using those values, the mechanism performance will be tested against molecular beam experimental data [10] on Pt(110).
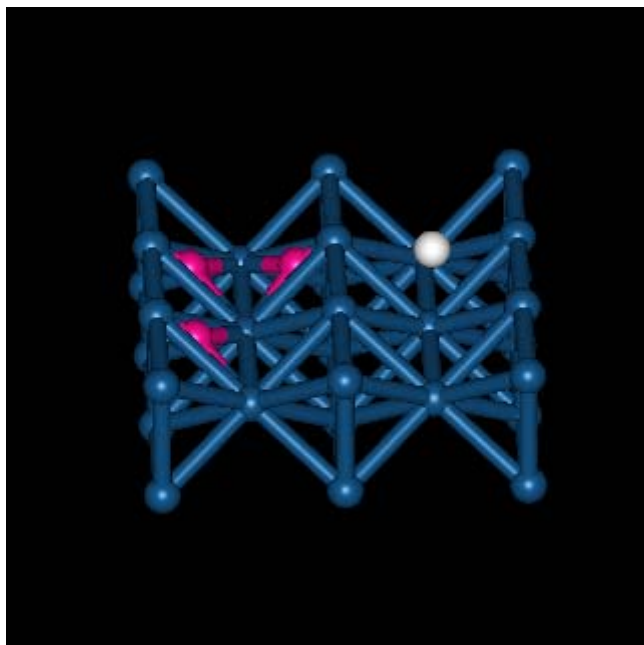
Figure 5.2: Picture of Pt (12,6,12) cluster with 30 Pt atoms. White sphere indicates a H-atom on a hollow site. The heats of chemisorptions Q are calculated using Gaussian 98 [11] and a basis set of 6-311G(d) as well as LANL pseudopotentials.

5.3.2 *Optimization of methane oxidation mechanism*

We focused on preliminary optimization of the methane surface reaction mechanism using the iterative optimization approach and SAB method [8]. CH_4 conversion, CO selectivity and H_2 selectivity data in a fluidized bed reactor [12] serve as targeted experiments. Predictions of the proposed unoptimized mechanism [3] are qualitatively in agreement with the experimental data, therefore, minimum adjustment of the mechanism parameters should predict the data quantitatively. We optimize pre-exponential factors only, keeping activation energies unchanged due to more confidence on DFT as well as BOC calculations. In the local sensitivity analysis, it is found that methane conversion is primarily affected by methane adsorption and desorption as well as H_2 adsorption and desorption, CO selectivity is primarily dependent on CO adsorption and desorption as well as CO_2 adsorption and desorption, whereas, H_2 selectivity is primarily sensitive to H_2 adsorption and desorption as well as H_2O adsorption and desorption steps. Polynomials are developed for all 3 types of data as a function of sensitive parameters at each iteration and finally distance between experimental data and the polynomial predictions is minimized using simulated annealing [9]. Fig. 5.3 shows the performance of the unoptimized mechanism as well as that of optimized mechanism [3]. CH_4 conversion as well as CO selectivity predictions are highly improved, whereas H_2 selectivity predictions are improved in the low temperature regime. The newly optimized parameters are presented in Table 4. It is seen that the performance of the mechanism can be improved with a minimal adjustment of parameters. We plan to further improve the performance of the mechanism with added steps involving oxygenates.
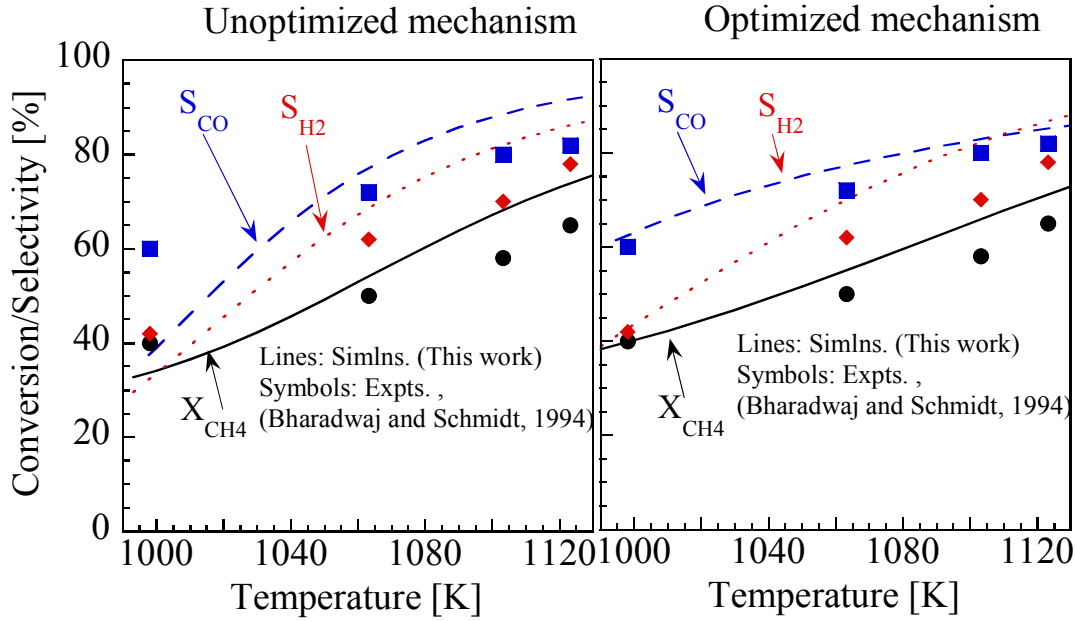
FIGURE 5.3: COMPARISON OF THE PERFORMANCE OF UNOPTIMIZED MECHANISM [3] AND OPTIMIZED MECHANISM [3] AGAINST EXPERIMENTAL DATA OF [12]. IMPROVEMENT IN THE PERFORMANCE IS OBSERVED FOR ALL TARGETS.

Table 5.4: Surface reaction mechanism for oxidation of methane on polycrystalline Pt. The activation energies are in kcal/mol, calculated at vacancy and oxygen dominated conditions.

No.	Reaction	k_f	E_f $\theta_*=1.$	E_f $\theta_{O*}=1$	k_b	E_b $\theta_*=1$	E_b $\theta_{O*}=.$
1	$OH*+* \leftrightarrow H*+O*$	$5.60\ 10^{11}$	24.4	18.3	$1.70\ 10^{10}$	12.1	13.4
2	$H_2O*+* \leftrightarrow H*+OH*$	$1.20\ 10^{10}$	18.4	39.1	$3.50\ 10^{11}$	12.4	0.0
3	$H_2O*+O* \leftrightarrow 2OH*$	$1.00\ 10^{11}$	12.6	34.1	$1.00\ 10^{11}$	18.9	0.0
4	$H_2+2* \leftrightarrow 2H*$	0.25 $0.09^@$	0.0	0.0	$1.00\ 10^{13}$ $3.33\ 10^{12@}$	20.0	20.0
5	$O_2+2* \leftrightarrow 2O*$	0.03^a	0.0	0.0	$1.00\ 10^{13a}$	51.0	19.0
6	$H_2O+* \leftrightarrow H_2O*$	0.70 $1.00^@$	0.0	0.0	$1.00\ 10^{13}$ $5.33\ 10^{12@}$	10.0	10.0
7	$OH+* \leftrightarrow OH*$	1.00	0.0	0.0	$1.00\ 10^{13}$	63.0	30.0
8	$H+* \leftrightarrow H*$	1.00	0.0	0.0	$1.00\ 10^{13}$	60.2	60.2
9	$O+* \leftrightarrow O*$	1.00	0.0	0.0	$1.00\ 10^{13}$	92.6	67.0
10	$CH_4+2* \leftrightarrow CH_3*+H*$	$1.00^{a,b}$ $0.68^@$	12.0	12.0	$1.00\ 10^{11}$ $3.97\ 10^{10@}$	5.5	5.5
11	$CH_3*+* \leftrightarrow CH_2*+H*$	$5.00\ 10^{12b}$	25.8	25.8	$1.00\ 10^{11}$	6.1	6.1

25

#	Reaction	A (a)	E (a)	E (a)	A (b)	E (b)	E (b)
		$1.32\ 10^{13@}$			$4.04\ 10^{10@}$		
12	$CH_2*+* \leftrightarrow CH*+H*$	$1.00\ 10^{11}$	25.0	25.0	$1.00\ 10^{11}$	12.2	12.2
13	$CH*+* \leftrightarrow C*+H*$	$1.00\ 10^{11}$	5.4	5.4	$1.00\ 10^{11}$	37.6	37.6
14	$CH_3*+O* \leftrightarrow CH_2*+OH*$	$1.00\ 10^{11}$	20.2	17.7	$1.00\ 10^{11}$	12.5	3.1
15	$CH*+OH* \leftrightarrow CH_2*+O*$	$1.00\ 10^{11}$	19.3	13.2	$1.00\ 10^{11}$	19.9	20.5
16	$C*+OH* \leftrightarrow CH*+O*$	$1.00\ 10^{11}$	45.9	38.2	$1.00\ 10^{11}$	1.5	1.5
17	$CH_2*+H_2O* \leftrightarrow CH_3*+OH*$	$1.00\ 10^{11}$	5.1	19.5	$1.00\ 10^{11}$	18.6	0.0
18	$CH*+H_2O* \leftrightarrow CH_2*+OH*$	$1.00\ 10^{11}$	13.2	26.7	$1.00\ 10^{11}$	19.5	0.0
19	$C*+H_2O* \leftrightarrow CH*+OH*$	$1.00\ 10^{11}$	38.1	70.9	$1.00\ 10^{11}$	0.1	0.0
20	$CO*+* \leftrightarrow C*+O*$	$1.00\ 10^{11}$	53.0	74.2	$1.00\ 10^{11}$	4.3	0.0
21	$CO_2*+* \leftrightarrow CO*+O*$	$1.00\ 10^{11}$	21.2	43.1	$1.00\ 10^{11}$	3.6	0.0
22	$CO+* \leftrightarrow CO*$	1.00 $0.71^{@}$	0.0	0.0	$1.00\ 10^{13}$ $1.21\ 10^{13@}$	34.0	34.0
23	$CO_2+* \leftrightarrow CO_2*$	1.00 $0.70^{@}$	0.0	0.0	$1.00\ 10^{13}$ $1.46\ 10^{12@}$	17.0	17.0
24	$CO_2*+H* \leftrightarrow CO*+OH*$	$1.00\ 10^{11}$	13.6	38.2	$1.00\ 10^{11}$	8.4	0.0
25	$CO*+H* \leftrightarrow CH*+O*$	$1.00\ 10^{11}$	80.5	106.	$1.00\ 10^{11}$	0.0	0.0
26	$CO*+H* \leftrightarrow C*+OH*$	$1.00\ 10^{11}$	40.3	69.2	$1.00\ 10^{11}$	4.0	0.0
27	$CH_3+* \leftrightarrow CH_3*$	1.00	0.0	0.0	$1.00\ 10^{13}$	38.0	38.0
28	$CH_2+* \leftrightarrow CH_2*$	1.00	0.0	0.0	$1.00\ 10^{13}$	68.0	68.0
29	$CH+* \leftrightarrow CH*$	1.00	0.0	0.0	$1.00\ 10^{13}$	97.0	97.0
30	$C+* \leftrightarrow C*$	1.00	0.0	0.0	$1.00\ 10^{13}$	150.	150.
31	$2CO* \leftrightarrow C*+CO_2*$	$1.00\ 10^{11}$ $2.40\ 10^{12@}$	31.0	31.0	$1.00\ 10^{11}$ $4.17\ 10^{09@}$	0.0	0.0

a: Optimized to predict ignition and extinction temperatures as inlet methane composition is varied.
b: Optimized to predict methane conversion and syngas selectivity as temperature is varied.
@: Iterative optimization for methane conversion and syngas selectivity.

5.3.3 References

1. Aghalayam, P., Park, Y. K. and Vlachos, D. G., AIChE J. 46(10): 2017-2029, This paper was selected in the highlights of Chem. Eng. Progress (paper of the month), p., Oct. issue, 2000. (2000).
2. Aghalayam, P., Park, Y. K. and Vlachos, D. G., Symposium (International) on Combustion 28: 1331-1339 (2000).
3. Aghalayam, P., Park, Y. K., Fernandes, N. E., Mhadeshwar, A. B., Vlachos, D. G. and Papavassiliou, V., J. Catalysis: Accepted (2002).
4. Shustorovich, E., Adv. Catal. 37: 101-164 (1990).
5. Shustorovich, E. and Sellers, H., Surf. Science Reports 31: 1-119 (1998).
6. Williams, W. R., Marks, C. M. and Schmidt, L. D., J. Phys. Chem. 96: 5922-5931 (1992).
7. van Santen, R. A. and Niemantsverdriet, J. W., Chemical kinetics and catalysis, Plenum Press, New York, 1995.
8. Davis, S. G., Mhadeshwar, A. B., Vlachos, D. G. and Wang, H., International Journal of Chemical Kinetics: Submitted (2002).
9. Kirkpatrick, S., Gelatt, C. D., Jr. and Vecchi, M. P., Science 220(4598): 671-680 (1983).
10. King, D. A. and Walker, A. V., J. Chem. Phys. B 104: 6462-6467 (2000).
11. Frisch, M. J., et al.: Gaussian, Inc., Pittsburgh PA, 2002
12. Bharadwaj, S. S. and Schmidt, L. D., J. Catal. 146: 11-21 (1994).

5.3.4 Publications resulted from this grant

1) A. B. Mhadeshwar, H. Wang, and D. G. Vlachos (2003) "Thermodynamic consistency in microkinetic development of surface reaction mechanisms", *J. Phys. Chem. B* **107**, 12721-12733.
2) A. B. Mhadeshwar, D. D. Kragten, and D. G. Vlachos, "Application of quantum mechanical density functional theory as a fundamental basis for microkinetic modeling of catalytic combustion", in *Third Joint Meeting of the U.S. Sections of The Combustion Institute*. 2003. Chicago, IL, Article, E02.
3) A. B. Mhadeshwar, P. Aghalayam, V. Papavassiliou, and D. G. Vlachos (2003) "Surface reaction mechanism development for platinum catalyzed oxidation of methane"*, Proc. Combust. Inst.* **29**, 997-1004.
4) S. Raimondeau, P. Aghalayam, A. B. Mhadeshwar, and D. G. Vlachos (2003) "Parameter optimization in molecular models: Application to surface kinetics", *Ind. Eng. Chem. Res.* **42**, 1174-1183.
5) S. G. Davis, A. B. Mhadeshwar, D. G. Vlachos, and H. Wang (2004) "A new approach to response surface development for detailed gas-phase and surface reaction kinetic model development and optimization"*, International Journal of Chemical Kinetics* **36**, 94-106.
6) P. Aghalayam, Y. K. Park, N. E. Fernandes, V. Papavassiliou, A. B. Mhadeshwar, and D. G. Vlachos (2003) "A C1 mechanism for methane oxidation on platinum", *J. Catal.* **213**, 23-38.

5.3.5 Oral presentations resulted so from this grant

1) B. Mhadeshwar, P. Aghalayam, V. Papavassiliou, and D. G. Vlachos, "Surface reaction mechanism development for partial oxidation of methane to synthesis gas", ACS meeting, Orlando, FL, April 7-11, 2002.

2) B. Mhadeshwar, P. Aghalayam, V. Papavassiliou, and D. G. Vlachos, "Surface reaction mechanism development for partial oxidation of methane to synthesis gas", *International symposium on combustion*, Sapporo, Japan, July 21-26, 2002.

5.3.6 *Poster presentations*

1) B. Mhadeshwar, and D. G. Vlachos, "Surface kinetics for methane partial oxidation: Mechanism development and automated optimization", CCST Research Review Meeting, University of Delaware, Newark, DE, Sept. 10, 2002.
2) B. Mhadeshwar, and D. G. Vlachos, "Surface kinetics for methane partial oxidation: Mechanism development and automated optimization", Philadelphia Catalysis Club meeting, Philadelphia, PA, Jan. 16, 2003.

5.3.7 *Invited talks*

1) "Recent advances in multiscale modeling of oxidation microreactors", Department of Mechanical and Aerospace Engineering, Univ. of Southern California, Los Angeles, CA, Feb. 13, 2002.
2) "Multiscale modeling: Application to materials nanotechnology and microreactors", Department of Mechanical and Industrial Engineering, Univ. of Illinois at Urbana-Champaign, IL, April 21, 2002.

6.   CONCLUSIONS

- Program achieved all of Phase I technical objectives

    – Thermal nozzle operation up to 40 atm

    – Mixing chamber operation up to 19atm

    – Catalyst chamber operation up to 19 atm

- Foster Wheeler completed economic estimates of base case and CHOR case

    – CHOR case is more economic than conventional technology

- A thermodynamically consistent theoretical reaction mechanism has been developed

- The economic advantage is not compelling and Praxair has decided to discontinue development